

Supramolecular Chemistry | Hot Paper |

Self-Assembly of a Tripod Aromatic Rod into Stacked Planar Networks

Ho-Joong Kim,^[b] Yongju Kim,^[a] Sung Cho,^[c] and Myongsoo Lee^{*[a]}

Abstract: Threefold symmetric rigid-core molecules with an internally grafted poly(ethylene oxide) (PEO) chain were synthesized, and their self-assembled structures were characterized using differential scanning calorimetry, TEM, and 1D and 2D X-ray scatterings in the solid state. The tripod compounds based on short PEO chains ($n=8, 13, 17, 21$), self-assemble into 2D channel-like network structures, whereas the compound with the longest PEO chain ($n=34$) forms a lamellar liquid crystalline phase. The interiors of the channel struc-

tures are filled with flexible PEO chains along the double-walled aromatic circumference. In these channel-like networks, three aromatic rods connected in the *meta*-position to each other are superimposed in parallel to other adjacent molecules to form the double-walled aromatic frameworks stacked perpendicular to the resulting channels. These are novel examples of supramolecular channel-like structures developed using amphiphilic diblock molecules based on a threefold symmetric rigid scaffold.

Introduction

The organization of well-defined organic nanostructures has been of great interest because of their potential in the creation of novel functional materials based on self-assembling systems.^[1] Among the diverse organic nanostructures, the development of channel-like structures has been one of the most important subjects in material science and polymer chemistry because of their application potential in electro-optic materials, ion channels, and lithograph processes.^[2] For instance, Percec and co-workers reported the fabrication of supramolecular channel-like structures such as porous columns and spheres with a hollow center at angstrom or nanometer scales using self-assembly of conical dendrons.^[3] Furthermore, these researchers developed non-hollow doubly segregated columns and vesicles or singly segregated columns with polyhedral shapes through modification at the apex of the dendrons.^[3e] The unique channel-like networks have been developed in liquid crystal (LC) states by Tschierske et al.^[4] These researchers demonstrated the formation of a series of channel-like structures with polygonal shapes from triangles via squares and pentagons to hexagons through a self-assembly process from polyphilic molecules. In these LC arrays, the polygonal ali-

phatic cylinders are separated by double-walled aromatic frameworks aligned perpendicular to the resulting channels. Kagome or honeycomb networks within a 2D crystal on a surface have been fabricated from π -conjugated cores substituted with alkyl chains.^[5]

Rod-coil diblock molecules consisting of rigid rod and flexible coil segments have emerged as promising candidates for the creation of well-defined supramolecular structures by a process of spontaneous organization.^[6] The morphological change of supramolecular nanostructures can be manipulated by elaborate control of the molecular structure and variation of the rod to coil volume fraction. Recently, we have demonstrated the preparation of 2D and 3D channel-like structures from the self-assembly of laterally grafted bent molecules with an oligoether chain at the internal bay position of the bent rods.^[7] Six bent molecules self-assemble into hexameric cycles through shape complementarity and aromatic stacking interactions, and then stack into channel-like columnar structures. Because the interior of the columns is occupied by the flexible chains, the 2D channels break up into discrete channels upon the elongation of an oligoether chain. In contrast to the bent rods connected by a flexible coil at the internal bay position, the incorporation of a flexible coil at the external apex of the bent rods leads to a vesicular columnar structure with an amorphous channel by a self-assembly process.^[8] In these vesicular structures, the inside of the channels is occupied by oligoether coils because part of the bent molecules is turned with their coil-attached apex facing inside.

As an extension of the previous bent molecules self-assembling into channel structures, the incorporation of a rod to a bent rod at the outer apex would produce threefold symmetric rigid molecules composed of three rods in the *meta*-position to each other, yielding a novel aromatic scaffold for the construction of networked channels.^[1m,n] In this article, we

[a] Dr. Y. Kim, Prof. Dr. M. Lee
State Key Laboratory for Supramolecular Structure and Materials
College of Chemistry, Jilin University, Changchun 130012 (China)
E-mail: mslee@jlu.edu.cn

[b] Dr. H.-J. Kim
Department of Chemistry, Chosun University, Gwangju 501-759 (Korea)

[c] Dr. S. Cho
Department of Chemistry, Chonnam National University
Gwangju 500-757 (Korea)

Supporting information for this article is available on the WWW under <http://dx.doi.org/10.1002/chem.201500780>.

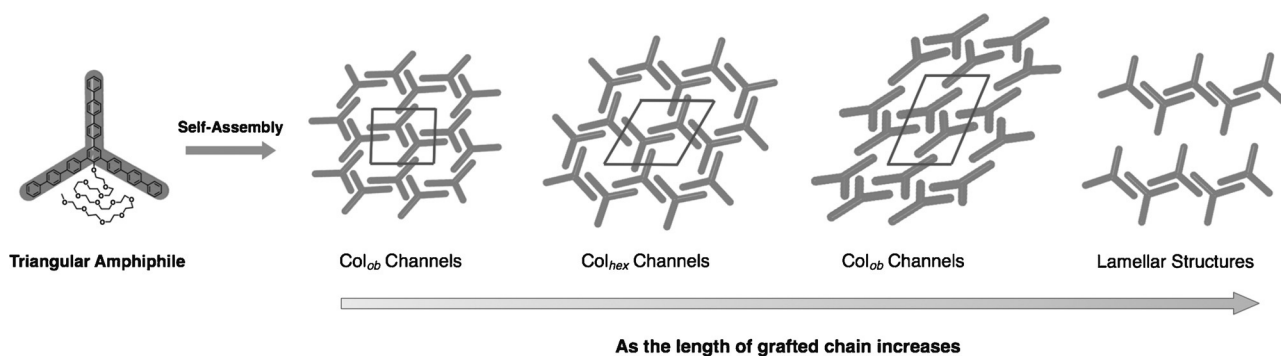


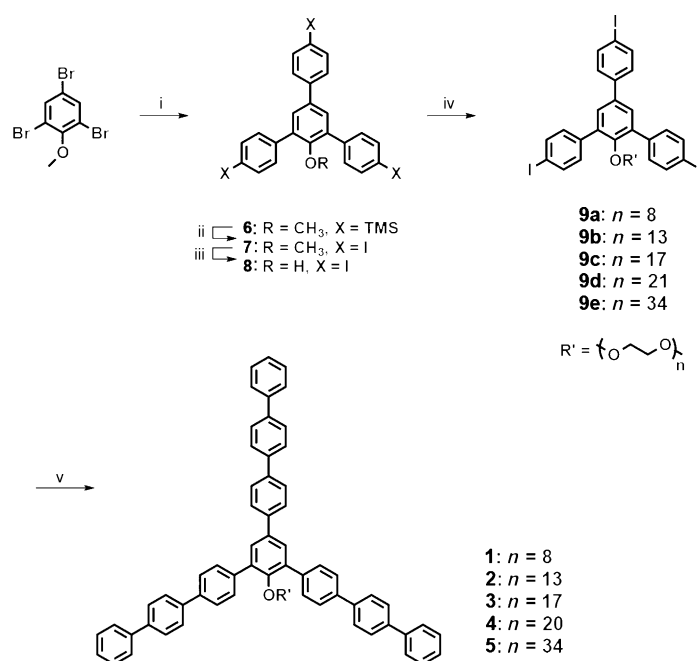
Figure 1. Schematic representation for self-assembled nanostructures from tripod amphiphiles 1–5. As the length of the attached chain increases, their self-assembled structures transform from oblique to hexagonal to oblique columnar channels, and finally to the lamellar LC structure.

report the synthesis of tripod rigid-flexible diblock molecules and the investigation of their self-assembled nanostructures using differential scanning calorimetry (DSC), TEM, and 1D and 2D X-ray scatterings in the solid states. The tripod diblock molecules consist of a threefold symmetric *p*-triphenylene-substituted benzene as a rigid segment and an internally attached poly(ethylene oxide) (PEO) chain as a coil segment. These amphiphiles self-assemble into various 2D channel-like network structures and a lamellar LC structure depending on the length of the incorporated PEO coils (Figure 1).

Results and Discussion

Scheme 1 describes the synthesis of compounds 1–5. The synthesis of the tripod amphiphiles was performed with the preparation of a threefold symmetric aromatic unit starting from a Suzuki coupling reaction with 2,4,6-tribromoanisole and trimethylsilyl-substituted phenyl boronic acids in the presence of a catalytic amount of tetrakis(triphenylphosphine) palladium(0). The introduction of the flexible chains was achieved by an etherification reaction of the corresponding tosylated PEO chain and the phenolic compound (**8**), and then Suzuki coupling reactions were performed with a biphenyl boronic acid, which yielded compounds 1–5. All the final compounds were characterized by NMR spectroscopy, elemental analysis, and matrix-assisted laser desorption time-of-flight (MALDI-TOF) mass spectrometry, and the resulting structures were shown to be in full agreement with the expected chemical structures.

The self-assembling behavior of the tripod amphiphiles in the bulk was investigated by using DSC and 1D and 2D X-ray scatterings. All the diblock molecules exhibited an ordered structure, and the transition temperatures were determined from DSC scans (Table 1 and Figure S1, Supporting Information). For compound **1** based on the shortest PEO chain ($n = 8$), the small-angle X-ray scattering (SAXS) pattern revealed several sharp reflections that could be indexed as a 2D oblique array with lattice constants of $a = 2.39$ nm, $b = 2.71$ nm together with a characteristic angle of 92° (Figure 2a). Based on the



Scheme 1. Synthesis Scheme of compounds 1–5. Reagents and conditions: i) 4-(trimethylsilyl)phenylboronic acid, tetrakis(triphenylphosphine) palladium(0), Na₂CO₃, H₂O/THF, reflux, 24 h; ii) ICl, methylene chloride, -78°C , 1 h; iii) BBr₃, methylene chloride, 0°C , 6 h; iv) poly(ethylene glycol) monomethylether monotosylate, K₂CO₃, acetonitrile, reflux, 24 h; v) 4-biphenylboronic acid, tetrakis(triphenylphosphine) palladium(0), Na₂CO₃, H₂O/THF, reflux, 24 h.

SAXS results and density, the number (N_{cell}) of molecules in a unit cell, defined as the lattice constants and an aromatic distance of 0.44 nm, could be calculated to be two.^[4d,9]

Considering that the N_{cell} is 2 and that the threefold-symmetry of aromatic segment in which the distance between the centered benzene ring and the peripheral hydrogen at the end of the aromatic rod is approximately 1.55 nm, we can conclude that the tripod molecules self-assemble into a channel-like network structure with an oblique shape in which the flexible PEO chains are filled inside the aromatic frameworks. In 2D planes, three aromatic rods connected with an angle of 120° are superimposed in parallel to other adjacent molecules to form the double-walled aromatic frameworks. Subsequently, the aromatic networks are stacked on top of each other and aligned verti-

Table 1. Phase transitions and lattice parameters of compounds of 1–5. ^[a]										
Compounds	<i>n</i>	Phase transition [°C] and corresponding enthalpy changes [kJ mol ⁻¹]	<i>a</i> [nm]	<i>b</i> [nm]	<i>d</i> [nm]	γ [°]	<i>A</i> [nm ²]	<i>V</i> _{cell} [nm ³]	<i>N</i> _{cell}	
1	8	Col _{ob} 205 (6.5) i i (5.3) 162 Col _{ob}	2.39	2.71	–	92	6.47	2.85	1.92	
2	13	Col _{hex} 197 (3.8) i i (4.0) 154 Col _{hex}	3.18	–	–	60	8.76	3.85	1.96	
3	17	Col _{ob} 178 (7.4) i i (6.3) 153 Col _{ob}	3.34	2.72	–	115.6	8.19	3.60	1.85	
4	21	Col _{ob} 171 (5.0) i i (4.3) 146 Col _{ob}	4.11	2.80	–	113	10.6	4.66	2.10	
5	34	Lam 161 (5.1) i i (6.1) 130 Lam	–	–	5.23	–	–	–	–	

[a] *n* = number of repeating units of PEO, *A* = cross-sectional area (nm²), Col_{ob} = oblique columnar channel in crystalline solid, Col_{hex} = hexagonal columnar channel in crystalline solid, Lam = lamellar liquid crystalline phase, i = isotropic liquid. DSC traces (peak temperatures, 5 °C min⁻¹) recorded during the second heating and first cooling scans. *N*_{cell} = number of molecules in the unit cell in the crystalline solid, calculated according to the following equation, $N_{\text{cell}} = \rho \times V_{\text{cell}} \times N_A / M$, where *M* is the molecular weight, ρ is density, *N*_A is Avogadro's number, and *V*_{cell} is the volume of unit cell defined by $a \times b \times \sin(\gamma) \times 0.44$ nm for Col_{ob} and $a^2 \times \sin(60^\circ) \times 0.44$ nm for Col_{hex}.^[4d,9] The height of unit cell was assumed to be 0.44 nm obtained from WAXS patterns indicative of the aromatic stacking distance. The densities were measured by flotation in a *n*-hexane/CCl₄ mixture.

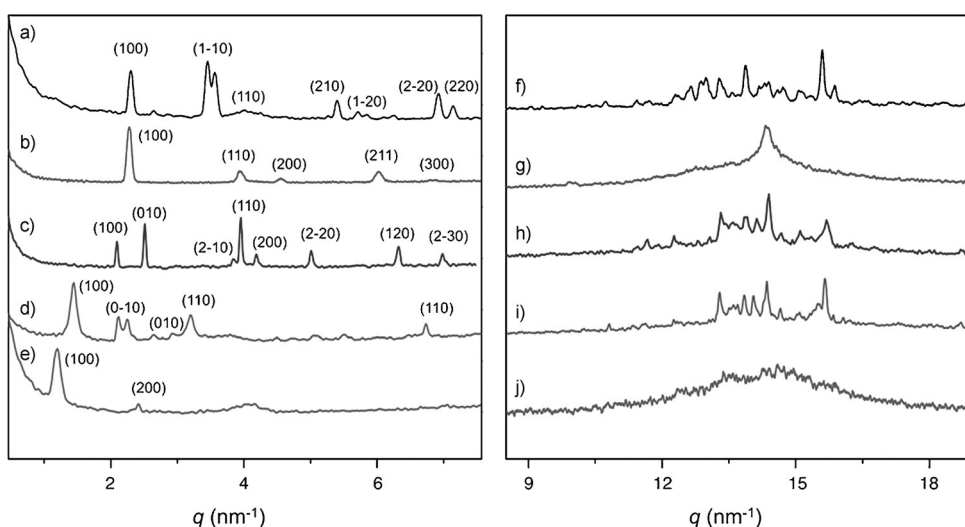


Figure 2. SAXS (a–e) and WAXS (e–j) patterns of compounds 1–5 against *q* ($q = 4\pi \sin 2\theta/\lambda$) at room temperature.

cal to the resulting channels with a 2D oblique array. The optimized structure of compound 1 revealed that the lattice constants of an oblique array only satisfy two molecules per unit cell within the suggested channel-like structures, which are separated by double-walled aromatic networks.

The SAXS reflections of compound 2 based on a longer PEO chain (*n* = 13) have a ratio of positions corresponding to 1:3^{1/2}:2:7^{1/2}:3, which indicates a hexagonal phase with a parameter *a* = 3.18 nm (Figure 2 a–e). The wide-angle X-ray scattering (WAXS) pattern of compound 2 revealed a sharp reflection that can be indexed as a π – π stacking distance of 0.44 nm (Figure 2 f–j). Using the observed lattice parameters, *N*_{cell} was calculated, yielding a value of two, which suggests that six aromatic rods form the circumference of the channels. Similar to the channel-like networks for compound 1, two rods are arranged in parallel within each of the walls separating the channel-like structure with a hexagonal shape in which the flexible PEO chains are filled inside. The length of the side forming the walls can be calculated according to $a/3^{1/2} = 1.8$ nm, which is consistent with the intermolecular distance between neighbor-

ing units of 1.77 nm based on the suggested double-walled network structure. The SAXS patterns of compounds 3 and 4 based on longer PEO chains (*n* = 17 and 20) can be indexed based on oblique columnar phases with the lattice parameters *a* = 3.34 and *b* = 2.72 nm and $\gamma = 115.6^\circ$ for 3 and *a* = 4.11 and *b* = 2.80 nm, and $\gamma = 113.1^\circ$ for 4 (Table 1). The calculated number of molecules per unit cell is 2, which is consistent with the suggested double-walled aromatic networks. The compounds 3 and 4 self-organize into oblique columnar channels consisting of flexible PEO chains inside and the double-walled aromatic segments along the circumference, similar to the structure observed for compounds 1 and 2. In addition, 2D XRD patterns of the channel structures revealed that the SAXS patterns are recorded vertically to the WAXS patterns, which indicates that the 2D channels stack through aromatic stacking perpendicular to the in-plane ordering (Figure 3).

The organized structure of 3 was further investigated by TEM, as shown in Figure 4. The image of an ultramicrotomed film of 3 stained with RuO₄ vapor revealed parallel columnar arrays which are spaced by approximately 2.7 nm, consistent with that obtained from X-ray scattering. The inset shows the top view image of the 2D columnar structure.

In contrast to compounds 1–4 based on short chains, compound 5 containing a longest flexible chain (*n* = 34) self-assembled into a layered structure, as confirmed by SAXS. The inter-

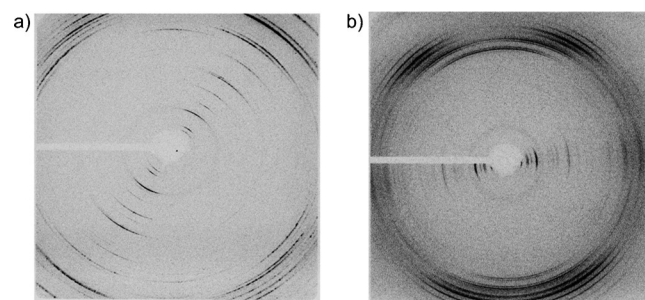


Figure 3. 2D XRD patterns of: a) 3 and b) 4 at room temperature.

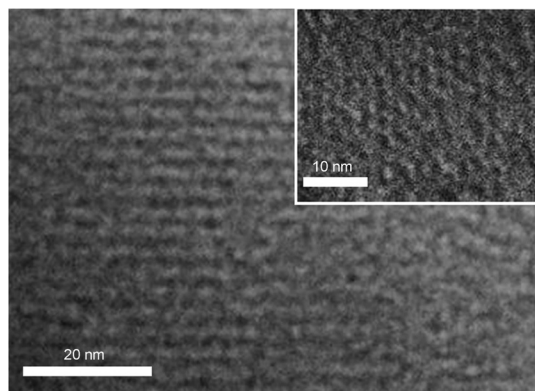


Figure 4. A representative TEM image of ultramicrotomed films of **3** stained with RuO_4 , revealing parallel columnar arrays. The inset image shows the top view of the columnar structure.

layer distance was observed to be 5.23 nm, which is consistent with the molecular length indicative of complete interdigitation of the chain segments. At the wide angle, only a diffused halo at $d=0.45$ nm remains as evidence of the lack of any positional long-range order, which indicates that compound **5** forms the disordered lamellar LC phase.

The notable feature of the SAXS patterns of **1–4** is the unusually strong high-order diffraction peaks of the channel-like structures. The enhanced diffraction peaks have been suggested to arise from the presence of a hollow or a core with low electron density, reflected in the appropriate shape of such reverse columns. For instance, the inverse hexagonal lyotropic LC phases containing water channels in the core exhibit enhanced higher order peaks.^[9] The LC arrays of polygonal networks or the vesicular double-segregated channels with aliphatic low electron density centers exhibit strong diffraction reflections.^[3,4,8] These enhanced high-order diffraction peaks suggest that the interiors of the columnar phases for compounds **1–4** are filled with PEO chains with relatively low density surrounded by aromatic walls.

As the length of the PEO chain increases, the cross-sectional areas within the unit cells of the oblique columnar channels increase from 6.47 for **1** to 8.19 for **3** to 10.6 nm² for **4**, which indicates that the volume of PEO segments contributes to the space filling the interior of the channels. To reduce the repulsive force between PEO chains, the channel structures are extended to allow more space for the bulky chains to adopt a less strained conformation. It can be deduced that the aromatic stackings must be tilted, yielding elliptical sections of the channels filled with PEO chains when viewed along the column axes with oblique arrangements. The oblique columnar channels of compounds **1**, **3**, and **4** exhibited many unassignable peaks at WAXS patterns, which indicate that the packing arrangement of rods is deformed because of the imbalance between the inner-size of the channel and the volume of the PEO chains. For compound **2**, the volume inside the hexagonal columnar channel appears to be suitable for the space available for the attached PEG ($n=13$), resulting in the efficient aromatic stackings. As illustrated in the WAXS pattern of compound **2**, there is a strong peak corresponding to an aromatic

stacking distance of 0.44 nm, which indicates that aromatic rods are stacked side-by-side effectively. If the length of the attached chains is further extended, then the PEOs in the channel fuses together to yield infinite layers because the PEO chain is too long to be surrounded by double-walled aromatic rods.

To explore the molecular origin of the channel-like networks, the molecular structures of the tripod amphiphiles were optimized by low (Hartree–Fock (HF) Hamiltonian with 3-21G basis set) to high level (density functional theory (DFT) B3LYP with 6-31G* basis set) in a stepwise manner (Figure 5). The overall

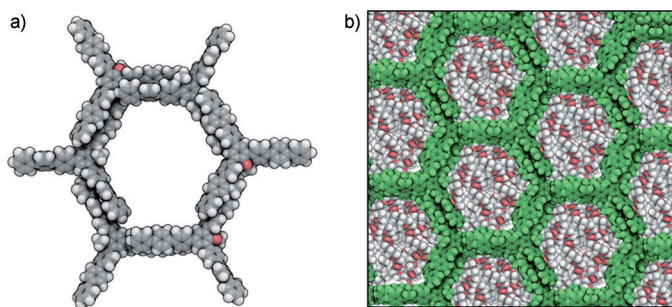


Figure 5. Snapshots of the channel structures of tripod molecules after MD calculation. a) Six tripod aromatic cores self-assemble into hexameric cycles with double-walled aromatic frameworks. b) The energetically optimized structure suggests that compound **2** with PEO ($n=13$) is suitable for the symmetric hexagonal columnar channels (the tripod aromatic cores are green).

shape of the optimized tripod amphiphiles is similar to a three-fold propeller at an angle of approximately 120°. Because the constituent phenyl units in each aromatic rod are coplanar (the average dihedral angle between them is $\sim 37^\circ$), the cores in the tripod amphiphiles can be accumulated by π – π interaction between aromatic rods. The energetically optimized structure suggests that compound **2** with PEO ($n=13$) is ideal for the symmetric hexagonal double-walled aromatic frameworks in which six tripod molecules in a single slice are packed into a shell of aromatic moieties, with two attached PEO chains inside the columns to fill the internal pore. These theoretical dimensional analyses are in good agreement with the results from XRD experiments.

This structural transformation is unexpected when compared with the previously reported 2D channel structures. For instance, the bolaamphiphiles consisting of a bent rod segment connected by glycerol units at the ends and an aliphatic chain in the lateral position self-assemble into various honeycomb channel-like structures through hydrogen bonds and π – π interactions.^[4] The hydrogen bonds, which provide strong cohesive forces between aromatic rods, can be broken with an increase in the volume of the aliphatic chains, which yields the packing-rearrangement of aromatic rods resulting in the different molecular number in the unit cells in contrast to the consistent value of two observed in our channel structures. It has also been reported that the channel structures based on bent molecules in the solid state break up into discrete channels

upon increasing the length of an oligoether chain.^[7b] The helical tubules from the bent amphiphiles in aqueous solution are segmented into sliced tubules while maintaining helical order in the discrete nanostructures upon the addition of hydrophobic alkyl counteranions.^[10] The unique structural change of the self-assembled channels from compounds **1–4** can be rationalized by considering that the individual channels are noncovalently bonded to each other by threefold symmetric rigid segments forming the aromatic network structures. Because the tripod aromatic core can act as a junction point by conjugating three adjacent channels, the resulting 3D interconnected aromatic stackings would prevent the breaking up of the channels along the *z*-axis. Instead, the aromatic frameworks are deformed maintaining the channel-like structures without sacrificing the π - π interactions.

Conclusion

Amphiphilic tripod molecules consisting of a threefold symmetric *p*-triphenylene-substituted benzene and a flexible PEO chain internally grafted in the aromatic core have been designed and used as building blocks for the fabrication of channel-like networks by a self-assembly process. The self-assembled channel structures are filled with flexible PEO chains inside the double-walled aromatic segments along the circumference. As the length of the attached chain increases, the supramolecular structures based on the tripod amphiphiles change from oblique to hexagonal to oblique columnar networks and finally to the lamellar LC structure. This result is attributed to the tripod structure, which provides combining junctions in the formation of aromatic networks resulting in the noncovalent conjugation of three adjacent channels. Using the novel tripod amphiphiles based on a threefold symmetric aromatic scaffold may be a useful strategy for the development of supramolecular channel-like networks.

Experimental Section

Materials

Tetrakis(triphenylphosphine) palladium(0) (99%), NaH (60%), and *p*-toluenesulfonyl chloride (98%) from TCI and Tokyo Kasei were used as received. 2,4,6-Tribromophenol, 4-biphenylboronic acid, iodine monochloride (1.0 M solution in dichloromethane), boron tribromide (1.0 M solution in dichloromethane) from Aldrich were used as received. Compound 4,4'-(trimethylsilyl) phenylboronic acid was prepared according to the similar procedures described previously. Unless otherwise indicated, all starting materials were obtained from commercial suppliers (Aldrich, Lancaster, and TCI, etc.) and were used without purification. Methylene chloride, hexane, and ethyl acetate were distilled before use. Visualization was accomplished with UV light and iodine vapor. Flash chromatography was carried out with Silica Gel 60 (230–400 mesh) from EM Science. Dry THF was obtained by vacuum transfer from sodium and benzophenone.

Equipment

¹H NMR spectra were recorded from CDCl₃ and DMSO solutions on a Bruker AM 250 spectrometer. The purity of the products was checked by thin layer chromatography (TLC; Merck, silica gel 60). MALDI-TOF mass spectra were performed on Perceptive Biosystems Voyager-DE STR using a α -cyano-4-hydroxycinnamic acid (CHCA) matrix. A Perkin-Elmer Diamond-DSC differential scanning calorimeter equipped with 1020 thermal analysis controller was used to determine the thermal transitions, which were reported as the maxima and minima of their endothermic or exothermic peaks. Compounds were synthesized according to the procedure described in Scheme 1 and then purified by silica gel column chromatography and prep. HPLC (Japan Analytical Instrument). X-ray scattering measurements were performed in transmission mode with synchrotron radiation at the 10C1 and 3C2 X-ray beam lines at Pohang Accelerator Laboratory, Korea. To investigate structural changes on heating, the sample was held in an aluminum sample holder, which was sealed with the window of 7 μ m thick Kapton films in both sides. The sample was heated with two cartridge heaters and the temperature of the samples was monitored by thermocouple placed close to the sample. The TEM was performed using JEOL HR-2100. The samples of untreated materials were microtomed by cryo-ultramicrotomy (Leica) and the resulting thin sections of samples were transferred to carbon-coated Cu-grid substrates. To improve mass thickness contrast and radiation sensitivity, the thin films were slightly exposed to staining agent vapor (0.5 wt.% aqueous RuO₄). Direct imaging was carried out at 120 kV accelerating voltage, using the images acquired with SC 1000 CCD camera (Gatan, Inc.; Warrendale, PA).

Synthesis

Compound 6: 2,4,6-Tribromoanisole (1.00 g, 2.90 mmol) and 4-(trimethylsilyl)phenylboronic acid (2.81 g, 14.5 mmol) were dissolved in degassed 2.0 M Na₂CO₃ aqueous solution (80 mL) and THF (50 mL). Then tetrakis(triphenylphosphine) palladium(0) (0.2 g, 0.2 mmol) was added. The mixture was heated at reflux for 24 h with vigorous stirring under nitrogen. Cooled to room temperature, the layers were separated, and the aqueous layer was then washed twice with ethyl acetate. The combined organic layer was dried over anhydrous magnesium sulfate and filtered. The solvent was removed in a rotary evaporator, and the crude product was purified by flash chromatography (silica gel) using hexane/methylene chloride (8:1, v/v) as the eluent to yield 1.3 g (81.1%) of white solid. ¹H NMR (250 MHz, CDCl₃): δ = 7.68–7.59 (m, 14H, Ar-H), 3.28 (s, 3H, OCH₃), 0.31 ppm (s, 18H, silane-CH₃).

Compound 7: A 1.0 M solution of ICl in methylene chloride (12 mL, 12 mmol) was added dropwise to a solution of **6** (1.3 g, 2.35 mmol) in distilled methylene chloride (300 mL) at -78°C . The reaction mixture was stirred over 1 h under nitrogen. Then, a 1.0 M aqueous Na₂S₂O₅ (100 mL) solution was added and stirred over 1 h at RT. The layers were separated and the aqueous layer was then washed twice with methylene chloride. The combined organic layer was dried over anhydrous magnesium sulfate and filtered. The solvent was removed by a rotary evaporator, and the crude product was purified by flash chromatography (silica gel) using ethyl acetate as eluent to yield 1.52 g (73%) of white powder. ¹H NMR (250 MHz, CDCl₃) δ = 7.78–7.74 (m, 6H, I-Ar-H, *J* = 4.8 Hz), 7.47 (s, 2H, Ar-H), 7.38–7.31 (m, 6H, I-Ar-H), 3.19 ppm (s, 3H, OCH₃).

Compound 8: BBr₃ (17.2 mL, 6.38 mmol) was added dropwise at 0 $^{\circ}\text{C}$ to a solution of **7** (1.52 g, 2.13 mmol) dissolved in dried methylene chloride (250 mL). The reaction mixture was stirred at room temperature under nitrogen for 6 h. The solution was quenched

with MeOH at 0 °C for 30 min. The crude product was filtered and dried to yield 1.32 g (88.5%) of a white solid. ¹H NMR (250 MHz, CDCl₃): δ = 7.84 (q, 4H, I-Ar-H), 7.76 (d, 2H, I-Ar-H), 7.43 (s, 2H, Ar-H), 7.33–7.30 ppm (m, 6H, I-Ar-H).

Compounds 9a–e: Compounds **9a–e** were synthesized by using the same procedure. A representative example is described for compound **9a**. Compound **8** (210 mg, 0.3 mmol), R-OTs (200 mg, 0.27 mmol) and excess K₂CO₃ were dissolved in acetonitrile (40 mL). The mixture was heated at reflux for 24 h and then cooled to room temperature. The mixture was poured into water and extracted with ethyl acetate, dried over anhydrous magnesium sulfate, and filtered. After the solvent was removed in a rotary evaporator, the crude products were purified by flash chromatography (silica gel) using methylene chloride and ethyl acetate/methanol (19:1 v/v) to yield 200 mg (88.9%) of a colorless liquid.

Data 9a: Yield: 88.9%; ¹H NMR (250 MHz, CDCl₃): δ = 7.79–7.74 (m, 6H, I-Ar-H, *J* = 8.4 Hz), 7.47 (s, 2H, Ar-H), 7.42–7.30 (m, 6H, I-Ar-H, *J* = 8.3 Hz), 3.90–3.37 (m, 32H, -OCH₂CH₂O-), 3.23 ppm (s, 3H, OCH₃); MALDI-TOF-MS: *m/z*: calcd: 1066.5 [*M*+H]⁺; found: 1066.3.

Data 9b: Yield: 84.7%; ¹H NMR (250 MHz, CDCl₃): δ = 7.78–7.75 (m, 6H, I-Ar-H, *J* = 8.4 Hz), 7.47 (s, 2H, Ar-H), 7.41–7.31 (m, 6H, I-Ar-H, *J* = 8.3 Hz), 3.91–3.36 (m, 52H, -OCH₂CH₂O-), 3.23 ppm (s, 3H, OCH₃); MALDI-TOF-MS: *m/z*: calcd: 1286.8 [*M*+H]⁺; found: 1286.5.

Data 9c: Yield: 56.9%; ¹H NMR (250 MHz, CDCl₃): δ = 7.78–7.75 (m, 6H, I-Ar-H, *J* = 8.4 Hz), 7.47 (s, 2H, Ar-H), 7.42–7.31 (m, 6H, I-Ar-H, *J* = 8.3 Hz), 3.91–3.36 (m, 68H, -OCH₂CH₂O-), 3.23 ppm (s, 3H, OCH₃); MALDI-TOF-MS: *m/z*: calcd: 1463.0 [*M*+H]⁺; found: 1462.8.

Data 9d: Yield: 88.4%; ¹H NMR (250 MHz, CDCl₃): δ = 7.79–7.74 (m, 6H, I-Ar-H, *J* = 8.4 Hz), 7.47 (s, 2H, Ar-H), 7.43–7.32 (m, 6H, I-Ar-H, *J* = 8.3 Hz), 3.90–3.37 (m, 84H, -OCH₂CH₂O-), 3.23 ppm (s, 3H, OCH₃); MALDI-TOF-MS: *m/z*: calcd: 1639.2 [*M*+H]⁺; found: 1638.9.

Data 9e: Yield: 83.4%; ¹H NMR (250 MHz, CDCl₃): δ = 7.79–7.74 (m, 6H, I-Ar-H, *J* = 8.4 Hz), 7.47 (s, 2H, Ar-H), 7.42–7.32 (m, 6H, I-Ar-H, *J* = 8.3 Hz), 3.90–3.36 (m, 136H, -OCH₂CH₂O-), 3.23 ppm (s, 3H, OCH₃); MALDI-TOF-MS: *m/z*: 2211.9 [*M*+H]⁺; found: 2211.6.

Compounds 1–5: Compounds **1–5** were synthesized using the same procedure. A representative example is described for compound **1**. Compound **9a** (0.350 g, 0.28 mmol) and 4-biphenylboronic acid (0.279 g, 1.41 mmol) were dissolved in degassed 2.0 M Na₂CO₃ aqueous solution (80 mL) and THF (50 mL). Then tetrakis(triphenylphosphine) palladium(0) (0.2 g, 0.2 mmol) was added. The mixture was heated at reflux for 24 h with vigorous stirring under nitrogen. Cooled to room temperature, the layers were separated, and the aqueous layer was then washed twice with ethyl acetate. The combined organic layer was dried over anhydrous magnesium sulfate and filtered. The solvent was removed in a rotary evaporator, and the crude product was purified by flash chromatography (silica gel) using methylene chloride as eluent. The solvent was removed in a rotary evaporator, and then purified by recycling GPC (Japan Analytical Industry) to yield 120 mg (62.2%) of white solid. ¹H NMR (250 MHz, CDCl₃): δ = 7.81–7.27 (m, 41H, I-Ar-H, Ar-H), 3.28 (s, 3H, OCH₃), 3.91–3.37 (m, 48H, OCH₂CH₂O), 3.23 ppm (s, 3H, OCH₃).

Data 1: Yield: 62.2%; ¹H NMR (250 MHz, CDCl₃): δ = 7.80–7.27 (m, 41H, I-Ar-H, Ar-H), 3.28 (s, 3H, OCH₃), 3.90–3.37 (m, 32H, OCH₂CH₂O), 3.23 ppm (s, 3H, OCH₃); elemental analysis: calcd: C 80.74, H 6.69; found: C 80.71, H 6.70; MALDI-TOF-MS: *m/z*: calcd: 1145.4 [*M*+H]⁺; found: 1145.2.

Data 2: Yield: 64.9%; ¹H NMR (250 MHz, CDCl₃): δ = 7.80–7.26 (m, 41H, I-Ar-H, Ar-H), 3.28 (s, 3H, OCH₃), 3.90–3.37 (m, 52H, OCH₂CH₂O), 3.23 ppm (s, 3H, OCH₃); elemental analysis: calcd: C

76.51, H 7.09; found: C 76.47, H 7.11; MALDI-TOF-MS: *m/z*: calcd: 1365.7 [*M*+H]⁺; found: 1365.5.

Data 3: Yield: 60.1%; ¹H NMR (250 MHz, CDCl₃): δ = 7.81–7.27 (m, 41H, I-Ar-H, Ar-H), 3.28 (s, 3H, OCH₃), 3.91–3.38 (m, 68H, OCH₂CH₂O), 3.23 ppm (s, 3H, OCH₃); elemental analysis: calcd: C 74.00, H 7.32; found: C 74.22, H 7.32; MALDI-TOF-MS: *m/z*: calcd: 1541.9 [*M*+H]⁺; found: 1541.6.

Data 4: Yield: 60.7%; ¹H NMR (250 MHz, CDCl₃): δ = 7.81–7.26 (m, 41H, I-Ar-H, Ar-H), 3.28 (s, 3H, OCH₃), 3.91–3.38 (m, 84H, OCH₂CH₂O), 3.23 ppm (s, 3H, OCH₃); elemental analysis: calcd: C 72.46, H 7.47; found: C 72.21, H 7.41; MALDI-TOF-MS: *m/z*: calcd: 1673.9 [*M*+H]⁺; found: 1674.3.

Data 5: Yield: 60.7%; ¹H NMR (250 MHz, CDCl₃): δ = 7.80–7.27 (m, 41H, I-Ar-H, Ar-H), 3.28 (s, 3H, OCH₃), 3.91–3.36 (m, 136H, OCH₂CH₂O), 3.23 ppm (s, 3H, OCH₃); elemental analysis: calcd: C 67.64, H 7.92; found: C 67.24, H 7.98; MALDI-TOF-MS: *m/z*: calcd: 2290.8 [*M*+H]⁺; found: 2290.6.

Acknowledgements

This work was supported by 1000 program, NSFC (grant 51473062 and grant 21450110416).

Keywords: channel nanostructure • planar network • self-assembly • supramolecular chemistry • tripod amphiphile

- [1] a) T. Shimizu, M. Masuda, H. Minamikawa, *Chem. Rev.* **2005**, *105*, 1401–1043; b) D. J. Hill, M. J. Mio, R. B. Prince, T. S. Hughes, J. S. Moore, *Chem. Rev.* **2001**, *101*, 3893–4012; c) F. J. M. Hoeben, P. Jonkheijm, E. W. Meijer, A. P. H. J. Schenning, *Chem. Rev.* **2005**, *105*, 1491–1546; d) Y. Yamamoto, T. Fukushima, Y. Suna, N. Ishii, A. Saeki, S. Seki, S. Tagawa, M. Taniguchi, T. Kawai, T. Aida, *Science* **2006**, *314*, 1761–1764; e) E. Yashima, K. Maeda, Y. Furusho, *Acc. Chem. Res.* **2008**, *41*, 1166–1180; f) J. M. Malicka, A. Sandeep, F. Monti, E. Bandini, M. Gazzano, C. Ranjith, V. K. Praveen, A. Ajayaghosh, N. Armadori, *Chem. Eur. J.* **2013**, *19*, 12991–13001; g) S. S. Babu, V. K. Praveen, A. Ajayaghosh, *Chem. Rev.* **2014**, *114*, 1973–2129; h) H. Cui, E. T. Pashuck, Y. S. Velichko, S. J. Weigand, A. G. Cheetham, C. J. Newcomb, S. I. Stupp, *Science* **2010**, *327*, 555–559; i) J. D. Hartgerink, E. Beniash, S. I. Stupp, *Science* **2001**, *294*, 1684–1688; j) D. Miyajima, K. Tashiro, F. Araoka, H. Takezoe, J. Kim, K. Kato, M. Takata, T. Aida, *J. Am. Chem. Soc.* **2009**, *131*, 44–45; k) J. J. van Gorp, J. A. J. M. Vekemans, E. W. Meijer, *J. Am. Chem. Soc.* **2002**, *124*, 14759–14769; l) F. García, L. Sanchez, *Chem. Eur. J.* **2010**, *16*, 3138–3146; m) A. Ajayaghosh, P. Chithra, R. Varghese, *Angew. Chem. Int. Ed.* **2007**, *46*, 230–233; *Angew. Chem.* **2007**, *119*, 234–237; n) P. Chithra, R. Varghese, K. P. Divya, A. Ajayaghosh, *Chem. Asian J.* **2008**, *3*, 1365–1373.
- [2] a) K. Tahara, S. Okuhata, J. Adisojoso, S. Lei, T. Fujita, S. DeFeyter, Y. Tobe, *J. Am. Chem. Soc.* **2009**, *131*, 17583–17590; b) M. Henmi, K. Nakatsujii, T. Ichikawa, H. Tomioka, T. Sakamoto, M. Yoshio, T. Kato, *Adv. Mater.* **2012**, *24*, 2238–2241; c) S. Ahn, A. J. Matzger, *J. Am. Chem. Soc.* **2010**, *132*, 11364–11371; d) N. Sakai, Y. Kamikawa, M. Nishii, T. Matsuoka, T. Kato, S. Matile, *J. Am. Chem. Soc.* **2006**, *128*, 2218–2219; e) M. R. Ghadiri, J. R. Granja, R. A. Milligan, D. E. McRee, N. Khazanovich, *Nature* **1993**, *366*, 324–327; f) D. T. Bong, T. D. Clark, J. R. Granja, M. R. Ghadiri, *Angew. Chem. Int. Ed.* **2001**, *40*, 988–1011; *Angew. Chem.* **2001**, *113*, 1016–1041; g) M. Reches, E. Gazit, *Science* **2003**, *300*, 625–627; h) M. Fritzsche, A. Bohle, D. Dudenko, U. Baumeister, D. Sebastiani, G. Richardt, H. W. Spiess, M. R. Hansen, S. Höger, *Angew. Chem. Int. Ed.* **2011**, *50*, 3030–3033; *Angew. Chem.* **2011**, *123*, 3086–3089.
- [3] a) V. Percec, A. E. Dulcey, V. S. K. Balagurusamy, Y. Miura, J. Smidral, M. Peterca, S. Nummelin, U. Edlund, S. D. Hudson, P. A. Heiney, D. A. Hu, S. N. Magonov, S. A. Vinogradov, *Nature* **2004**, *430*, 764–768; b) M. A. Shcherbina, X. B. Zeng, T. Tadjiev, G. Ungar, S. H. Eichhorn, K. E. S. Phillips, T. J. Katz, *Angew. Chem. Int. Ed.* **2009**, *48*, 7837–7840; *Angew. Chem.* **2009**, *121*, 7977–7980; c) V. Percec, A. E. Dulcey, M. Peterca, M. Ilies,

- M. J. Sienkowska, P. A. Heiney, *J. Am. Chem. Soc.* **2005**, *127*, 17902–17909; d) V. Percec, M. Peterca, A. E. Dulcey, M. R. Imam, S. D. Hudson, S. Nummelin, P. Adelman, P. A. Heiney, *J. Am. Chem. Soc.* **2008**, *130*, 13079–13094; e) M. Peterca, M. R. Imam, P. Leowanawat, B. M. Rosen, D. A. Wilson, C. J. Wilson, X. Zeng, G. Ungar, P. A. Heiney, V. Percec, *J. Am. Chem. Soc.* **2010**, *132*, 11288–11305.
- [4] a) M. Prehm, F. Liu, U. Baumeister, X. Zeng, G. Ungar, C. Tschierske, *Angew. Chem. Int. Ed.* **2007**, *46*, 7972–7975; *Angew. Chem.* **2007**, *119*, 8118–8121; b) X. Cheng, X. Dong, G. Wei, M. Prehm, C. Tschierske, *Angew. Chem. Int. Ed.* **2009**, *48*, 8014–8017; *Angew. Chem.* **2009**, *121*, 8158–8161; c) X. B. Zeng, R. Kieffer, B. Glettner, C. Nürnberger, F. Liu, K. Pelz, M. Prehm, U. Baumeister, H. Hahn, H. Lang, G. A. Gehring, C. H. M. Weber, J. K. Hobbs, C. Tschierske, G. Ungar, *Science* **2011**, *331*, 1302–1306; d) F. Liu, B. Chen, B. Glettner, M. Prehm, M. K. Das, U. Baumeister, X. Zeng, G. Ungar, C. Tschierske, *J. Am. Chem. Soc.* **2008**, *130*, 9666–9667; e) X. Tan, L. Kong, H. Dai, X. Cheng, F. Liu, C. Tschierske, *Chem. Eur. J.* **2013**, *19*, 16303–16313.
- [5] a) K. Tahara, S. Lei, J. Adisojoso, S. De Feyter, Y. Tobe, *Chem. Commun.* **2010**, *46*, 8507–8525; b) S. Furukawa, H. Uji-i, K. Tahara, T. Ichikawa, M. Sonoda, F. C. De Schryver, Y. Tobe, S. De Feyter, *J. Am. Chem. Soc.* **2006**, *128*, 3502–3503.
- [6] a) M. Lee, B.-K. Cho, W.-C. Zin, *Chem. Rev.* **2001**, *101*, 3869–3892; b) M. Lee, Y.-S. Jeong, B.-K. Cho, N.-K. Oh, W.-C. Zin, *Chem. Eur. J.* **2002**, *8*, 876–883; c) H.-J. Kim, T. Kim, M. Lee, *Acc. Chem. Res.* **2011**, *44*, 72–82; d) D.-J. Hong, E. Lee, H. Jeong, J.-K. Lee, W.-C. Zin, T. D. Nguyen, S. C. Glotzer, M. Lee, *Angew. Chem. Int. Ed.* **2009**, *48*, 1664–1668; *Angew. Chem.* **2009**, *121*, 1692–1696; e) D.-J. Hong, E. Lee, J.-K. Lee, W.-C. Zin, M. Han, E. Sim, M. Lee, *J. Am. Chem. Soc.* **2008**, *130*, 14448–14449.
- [7] a) Z. Huang, S.-K. Kang, M. Banno, T. Yamaguchi, D. Lee, C. Seok, E. Yamashita, M. Lee, *Science* **2012**, *337*, 1521–1526; b) H.-J. Kim, Y.-H. Jeong, E. Lee, M. Lee, *J. Am. Chem. Soc.* **2009**, *131*, 17371–17375.
- [8] H.-J. Kim, F. Liu, J.-H. Ryu, S.-K. Kang, X. Zeng, G. Ungar, J.-K. Lee, W.-C. Zin, M. Lee, *J. Am. Chem. Soc.* **2012**, *134*, 13871–13880.
- [9] a) H.-J. Kim, W.-C. Zin, M. Lee, *J. Am. Chem. Soc.* **2004**, *126*, 7009–7014; b) X. Cheng, F. Liu, X. Zeng, G. Ungar, J. Kain, S. Diele, M. Prehm, C. Tschierske, *J. Am. Chem. Soc.* **2011**, *133*, 7872–7881.
- [10] a) D. C. Turner, S. M. Gruner, *Biochemistry* **1992**, *31*, 1340–1355; b) M. Rappolt, A. Hickel, F. Bringezu, K. Lohner, *Biophys. J.* **2003**, *84*, 3111–3122.
- [11] H.-J. Kim, S.-K. Kang, Y.-K. Lee, C. Seok, J.-K. Lee, W.-C. Zin, M. Lee, *Angew. Chem. Int. Ed.* **2010**, *49*, 8471–8475; *Angew. Chem.* **2010**, *122*, 8649–8653.

Received: February 26, 2015

Revised: June 3, 2015

Published online on July 6, 2015